

Characterization and Application of Mangosteen Peel Activated Carbon for Ammonia Gas Removal

Zarah Arwieny Hanami* and Puji Lestari

Faculty of Civil and Environmental Engineering, Bandung Institute of Technology, Bandung 40132, Indonesia

ARTICLE INFO

Received: 9 Jan 2021
Received in revised: 3 May 2021
Accepted: 21 May 2021
Published online: 10 Jun 2021
DOI:10.32526/enrj/19/2020298

Keywords:

Activated carbon/ Adsorption/
Ammonia/ Mangosteen peel

* Corresponding author:

E-mail:
zaraharwienyhanami@gmail.com

ABSTRACT

Mangosteen peel can be used as an activated carbon precursor because of its high lignin content and hardness. In this study, mangosteen peel activated carbon (MP-AC) was prepared by a physical activation method using CO₂ at 850°C. The Brunauer-Emmett-Teller (BET) analysis was used to assess the optimal activation time to identify the largest surface area. The properties of MP-AC were characterized by the SEM-EDS and FTIR analyses. The results showed that MP-AC obtained from the 120-minute activation time had the largest BET specific surface area of 588.41 m²/g and was selected as an adsorbent in the dynamic adsorption of ammonia gas. The values of moisture content, ash content, and iodine number of MP-AC were 6.07%, 9.8%, and 1153.69 mg/g, respectively. Breakthrough curve indicated that with lower inlet concentration and higher adsorbent mass, longer breakthrough time is reached. Equilibrium data was best fitted to the Langmuir isotherm, while the pseudo-first order kinetic model favorably described the adsorption kinetics. The results revealed a potential to utilize MP-AC as an adsorbent for ammonia gas removal with average NH₃ adsorption capacity of 0.41 mg/g.

1. INTRODUCTION

Ammonia (NH₃) is a colorless gas with pungent odor which is emitted from agriculture, fertilizer industry, fossil fuel combustion, and some chemical industries (Vohra, 2020). The typical NH₃ concentrations emitted from the industrial process can range from 5 to 60 ppm (Chung et al., 2001) and ammonia from agricultural activities comprises approximately 80%-90% of total anthropogenic ammonia emissions (Xu et al., 2019). Ammonia is a threat to the environment due to its contribution to aerosol (PM_{2.5}) formation that could adversely affect respiratory and cardiovascular systems, and its deposition leads to eutrophication, acidification, and loss of biodiversity (Xu et al., 2019).

Adsorption using activated carbon is a simple and low-cost method (Guo et al., 2005) to purify NH₃. Many reports have described the adsorption of ammonia gas by activated carbon (Domingo-Garcia et al., 2002; Ro et al., 2015; Vohra, 2020). This adsorption process depends on some factors such as the pore size, area, and surface chemistry (Bernal et al., 2018). Lignocellulosic agricultural wastes with

their abundant availability, biodegradability, and non-toxic nature (Crini and Lichtfouse, 2018) can be used as an ideal precursor to produce activated carbon due to its high carbon content from the lignin composition (Nor et al., 2013). Several studies that used fruit peels for activated carbon productions such as durian peel (Chandra et al., 2009), rambutan peel (Ahmad and Alrozi, 2011), orange peel (Fernandez et al., 2014), and mangosteen peel (Nasrullah et al., 2019) have been conducted, and mangosteen peel has the highest lignin content of 48.63% (Devi et al., 2012).

Mangosteen (*Garcinia mangostana* L.) is a fruit largely found in Indonesia. The production in 2018 reached 228,155 tons which increased 41.05% from the previous year (Statistics Indonesia, 2019). This mass production leads to the peel waste increase (Rattanapan et al., 2014) where, according to Foo and Hameed (2012) and this study, about 60-70% of 1 kg of mangosteen fruit is the peel. Mangosteen peel can be used as an activated carbon precursor because it hardens when exposed to air thus making it suitable for granular activated carbon productions, has high lignin content (Devi et al., 2012) and low volatile

Citation: Hanami ZA, Lestari P. Characterization and application of mangosteen peel activated carbon for ammonia gas removal. Environ. Nat. Resour. J. 2021;19(4):320-329. (<https://doi.org/10.32526/enrj/19/2020298>)

substances, and it has porous properties comparable to commercial activated carbon (Chen et al., 2011).

Physical activation using carbon dioxide (CO₂) has advantages such as creating narrower pores, being easy to control, inexpensive, and environmentally safe (Ahmad et al., 2013; Rangabhashiyam and Balasubramanian, 2019). However, the use of CO₂ activation for mangosteen peel activated carbon (MP-AC) is rarely reported. Mukti et al. (2015) was using steam activation, while other studies were using chemical activation (Rattanapan et al., 2014; Nasrullah et al., 2019). Although the effectiveness of mangosteen peel as an adsorbent in CO₂ and ethylene gas adsorption (Giraldo and Moreno-Piraján, 2017; Mukti et al., 2015) is accepted, none has assessed the MP-AC for the NH₃ adsorption. This study aims to characterize MP-AC prepared by CO₂ activation for NH₃ gas removal. Dynamic adsorption was used to illustrate the real conditions in the environment (Meneghetti et al., 2010; Patel, 2019) where emitted gas moves continuously through the bed. The adsorption capacities, kinetics, and isotherm were also investigated in this study. The results may provide necessary theoretical guidance of this material using physical activation method and implementation in the gas-phase dynamic adsorption.

2. METHODOLOGY

2.1 Adsorbent preparation

Mangosteen peels collected from the market were washed with distilled water and then dried at 105°C for 24 h (Li et al., 2018) before they were crushed using roll crushing machine and mortar grinder RM 200, and sieved into 10-20 mesh size. The carbonization was conducted in a tube furnace, Carbolite Gero HST 12/600 + 301 Controller, with a temperature of 700°C for 3 h under the flow of nitrogen (N₂) gas. The process continued with CO₂ activation under N₂ atmosphere at 850°C for 15, 120, and 180 min. The ramping rate for carbonization and activation process was 10°C/min. The purity of CO₂ and N₂ gases used in this study was industrial grade ≥99% from PT. Aneka Gas Industri.

2.2 Activated carbon characterization

The Brunauer-Emmett-Teller (BET) analysis (Quantachrome Nova Ver 11.0) carried out to determine the surface area through nitrogen adsorption experiment at the temperature of 77 K (-196.15°C). Scanning Electron Microscope-Energy Dispersive Spectroscopy (SEM-EDS, Analytical SEM JEOL

JSM-6510A) was used to determine the morphological and elemental composition of MP-AC. The surface functional group was also determined using FTIR spectroscopy (IRPrestige-21 Shimadzu) at the wave interval of 4,000 and 340 cm⁻¹.

Moisture content, ash content, and iodine adsorption were determined according to the Indonesian standard, SNI 06-3730-1995 (Hastuti et al., 2015). The moisture content test was done by drying 1 g of the MP-AC at 105°C until the constant mass. The MP-AC was heated in the furnace at 600°C for 4 h to determine the ash content. Meanwhile, the iodine number test was performed by mixing 0.5 g of MP-AC with 50 mL of 0.1 N of iodine solution for 15 min. The filtrate (10 mL) was then titrated with 0.1 N of sodium thiosulfate solution and starch as an indicator. The equations used were as follows:

$$\% \text{Moisture content} = \frac{a-b}{a} \times 100\% \quad (1)$$

$$\% \text{Ash content} = \frac{b}{a} \times 100\% \quad (2)$$

$$\text{Iodine number } \left(\frac{\text{mg}}{\text{g}} \right) = \frac{(V_1 N_1 - V_2 N_2) \times 126.93 \times fp}{W} \quad (3)$$

Where; a and b are initial and final mass of activated carbon (g) respectively; V₁ is the analyzed iodine volume (mL); V₂ is the volume of Na₂S₂O₃ used (mL); W is activated carbon weight (g); N₁ and N₂ are the iodine and Na₂S₂O₃ normality (N) respectively; fp is the dilution factor; and 126.93 is the iodine amount corresponding to 1 mL of Na₂S₂O₃ solution.

2.2 Adsorbate preparation

An analytical grade stock solution of ammonia (NH₄OH) was prepared in this study to make artificial gas by aerating dilute ammonia solution (Yani et al., 2013) with an air flow of 880 mL/min for 30 min. The NH₃ gas was produced and collected in a polyethylene bag with a volume capacity of 120 L.

2.3 Adsorption experiment

Dynamic adsorption experiments were conducted in the laboratory using the Duran glass column (diameter=1.2 cm, height=40 cm). The NH₃ gas was injected into the column at a flow rate of 1.1 L/min. The outlet gas was measured by a gas sensor SKY2000-M2 at intervals of one reading per minute. The test was carried out continuously until the adsorbent reached saturated condition. The schematic diagram for the adsorption test is presented in Figure 1.

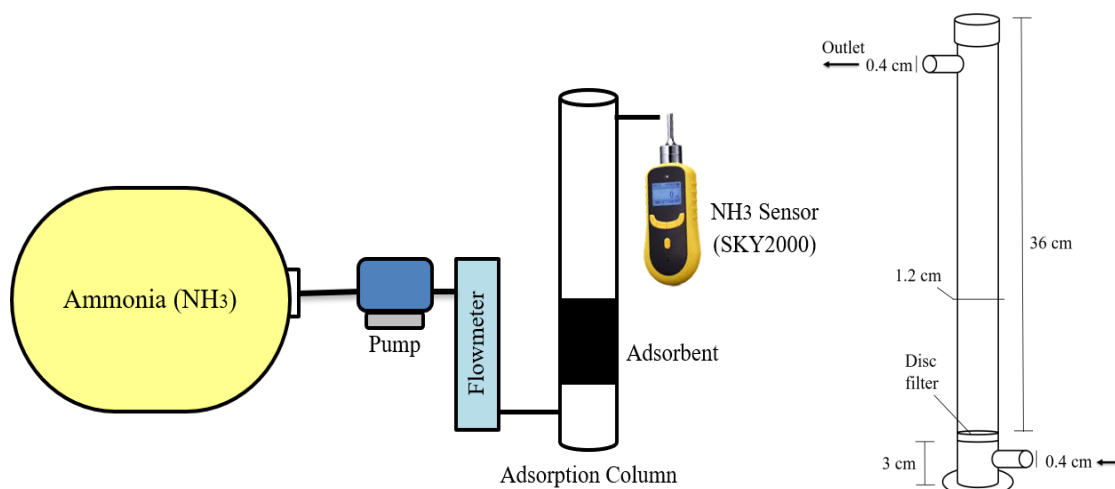


Figure 1. Illustration of the adsorption system test

The variations used in NH_3 adsorption process were adsorbent mass (1, 3, and 5 g) and initial NH_3 concentrations (10 ± 1 , 20 ± 1 , and 40 ± 1 ppm). Data were collected twice for each variation and the adsorption capacity was calculated using equation 4 (Choo et al., 2013):

$$q \left(\frac{\text{mg}}{\text{g}} \right) = \frac{(C_0 - C_t) \text{ mg/L} \times \text{Flowrate (L/min)} \times t \text{ (min)}}{\text{Adsorbent mass (g)}} \quad (4)$$

Where; t is the equilibrium time, C_0 and C_t are the gas inlet and outlet concentrations.

Activated carbon used in this study were disposed to the waste management and treatment facility by following applicable rules or can be regenerated using thermal, steam, and chemical processes (Reza et al., 2020).

3. RESULTS AND DISCUSSION

3.1 BET analysis and activation time selection

Microporosities and surface area are important properties that characterize carbon adsorbents (Saputro et al., 2020). The results of BET analysis at various activation times are shown in Figure 2.

Figure 2 shows that the surface area increased from $39.06 \text{ m}^2/\text{g}$ to $588.41 \text{ m}^2/\text{g}$ with activation times of 15 and 120 min, respectively, and then decreased to $535.62 \text{ m}^2/\text{g}$ with longer activation time (180 min). In the activation process, superheated CO_2 diffuses into the inner precursor which burns the blockage of the byproducts, expands the pore, and increases the surface area (Lan et al., 2019; Yuliusman et al., 2017). The activation reaction can be seen below (Cheremisinoff dan Ellerbusch, 1978).

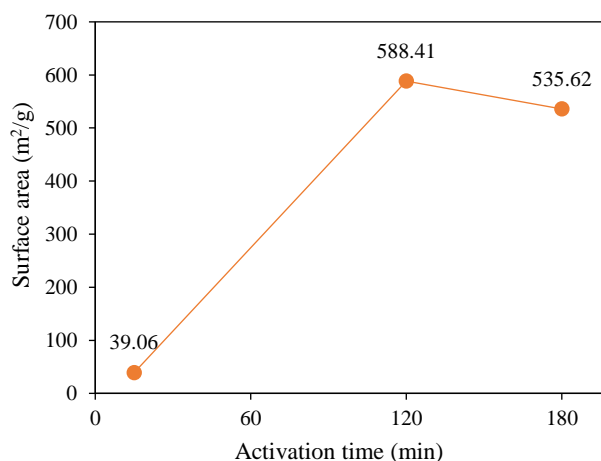
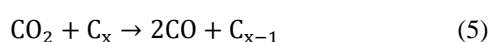


Figure 2. MP-AC surface area at various activation times.

According to Yang and Lua (2003), the increase in activation time increases the BET surface area. However, it can also result in the excessive carbon- CO_2 reaction, thus causing the expansion of the pores and some pore walls to collapse. Therefore, the surface area decreases in 180 min, and 120 min was chosen as the optimum activation time used in this study. The surface area obtained is smaller compared to the previous MP-AC studies using steam and chemical activation (Mukti et al., 2015; Nasrullah et al., 2019), probably due to the temperature and activating agent being used (Gebreegziabher et al., 2019). However, the surface area of activated carbon usually ranges $300\text{--}2,000 \text{ m}^2/\text{g}$ (Saputro et al., 2020), meaning that the result is still in the suitable range.

The isotherm graph obtained (Figure 3) showed the BET type 1 according to IUPAC classification, which usually indicates that the material is micro-shaped (Ambroz et al., 2018) with a relatively broad range of pore size distributions including wider and

narrower micropores ($< \sim 2.5$ nm) (Giraldo and Moreno-Pirajan, 2018).

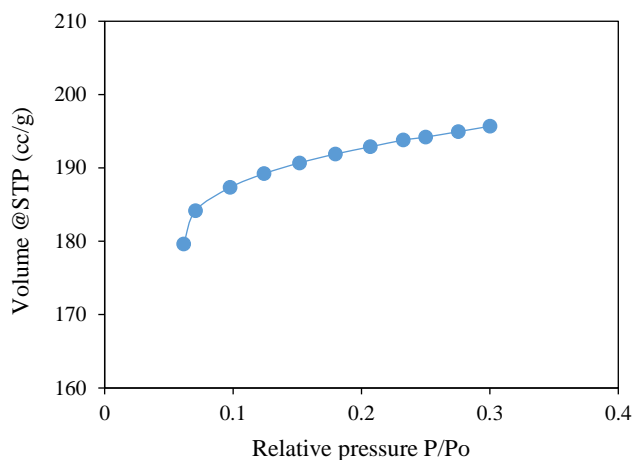


Figure 3. BET isotherm graph

Table 1. Characterization of MP-AC

Activation/temperature (°C)	Moisture content (%)	Ash content (%)	Iodine number (mg/g)	References
Physical CO ₂ /850	6.07	9.8	1153.69	This research
Chemical ZnCl ₂ 600	4.8	1.45	N/A	Nasrullah et al. (2019)
Chemical ZnCl ₂	1.07	5.68	820	Rattanapan et al. (2014)
Physicochemical KOH-CO ₂ /828	9.08	1.63	N/A	Ahmad and Alrozi (2010)

The iodine number obtained is 1153.69 mg/g, higher than that of Rattanapan et al. (2014). This iodine number shows adsorption ability, illustrates the porosity of activated carbon, and its higher value attributed to the presence of micropores as already proven in the BET isotherm graph. The result is also

3.2 Characterization of mangosteen peel activated carbon

The results of moisture, ash content, and iodine number compared to other studies are shown in Table 1.

Based on Table 1, the moisture content (6.07%) is higher than other studies' which use chemical activation, and lower than that of using physicochemical activation. This content indicates the hygroscopic nature which can affect the adsorption capacity (Hastuti et al., 2015). Meanwhile, the ash content which indicates the mineral content in activated carbon (Hastuti et al., 2015) has the highest value (9.8%) of all. According to Rangabhashiyam and Balasubramanian (2019), it can be influenced by the pyrolysis temperature and the activation method. The physical activation has a lower efficiency in reducing the mineral content than chemical activation, so the ash content becomes relatively higher.

included in the range of suitable activated carbon (500-1,200 mg/g) (Saka, 2012).

3.3 FTIR and SEM-EDS analyses

The surface functional group of MP-AC is characterized using FTIR as seen in Figure 4.

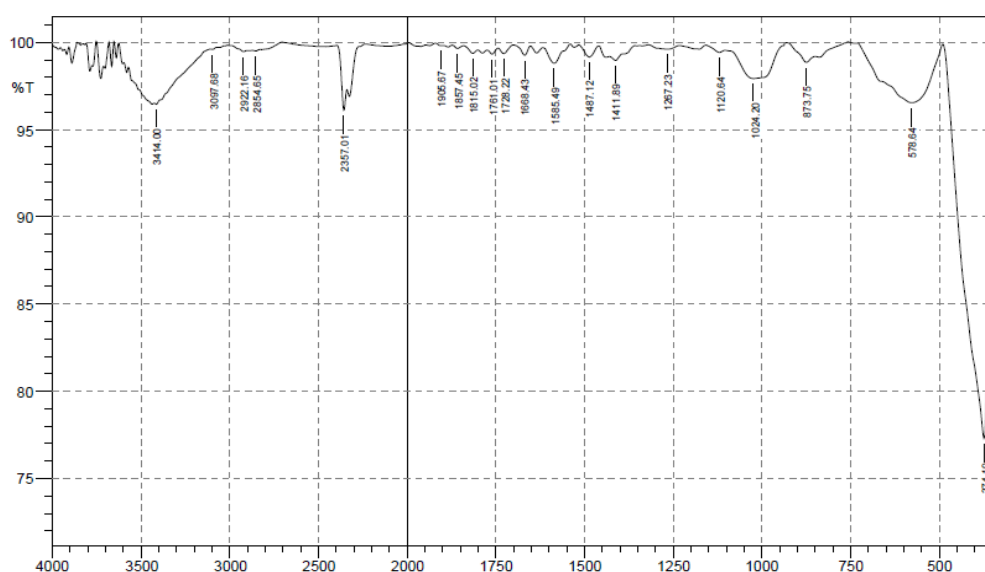


Figure 4. FTIR characterization spectrum of MP-AC

The FTIR result (Figure 4) shows many peaks which representing the complex nature of MP-AC (Nasrullah et al., 2019). The broad peak in 3,600-3,200 cm^{-1} indicates the presence of hydroxyl (O-H) group influenced by CO_2 as an activating agent, and the peak in 2,400-2,300 cm^{-1} shows a formation of nitrile ($\text{C}\equiv\text{N}$) (Ahmad et al., 2013). The small peak that occurs in 1,267.23 cm^{-1} and 1,120.64 cm^{-1} indicates the MP-AC contains a lack of C-O stretching as oxygen

functional group in lactonic groups, alcoholic groups, and carboxylate moieties (Chen et al., 2011; Nasrullah et al., 2019). Moreover, the peaks in range of 1,620-1,400 cm^{-1} , 1,760-1,690 cm^{-1} , 3,100-2,850 cm^{-1} , and <900 cm^{-1} , indicates C=C stretching, carbonyl group C=O, hydrocarbons C-H, and aromatic bond C-H, respectively (Ahmad et al., 2013).

The results of SEM analysis before and after the adsorption process can be seen in Figure 5 as follows

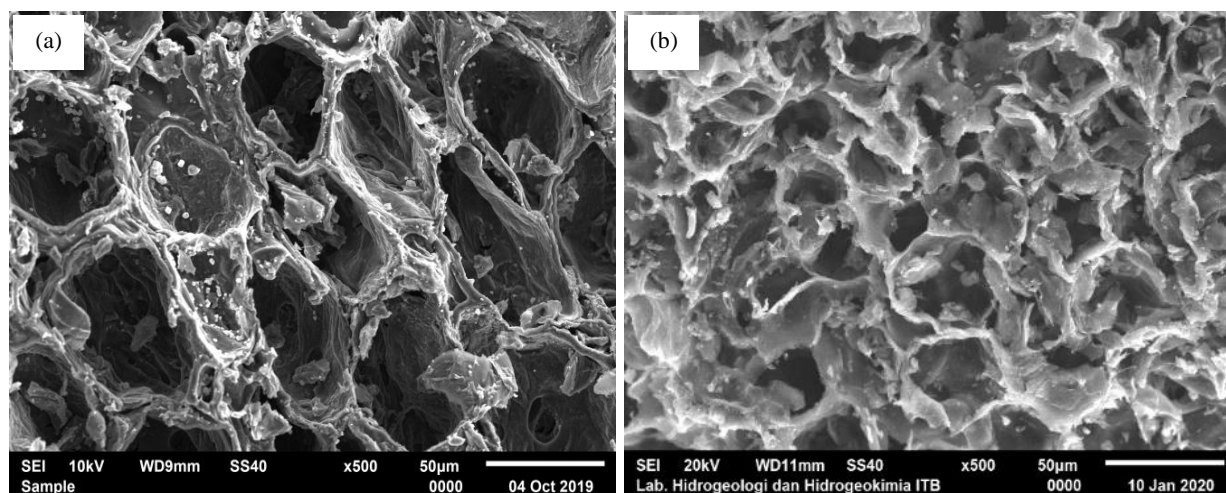


Figure 5. SEM image (a) before; (b) after NH_3 adsorption

Before adsorption (Figure 5(a)), morphology shows presence of circular pores in different size and crevices after the carbonization and CO_2 activation. It is shown that the MP-AC has porous nature that might affect the adsorption process (Nasrullah et al., 2019). After the adsorption (Figure 5(b)) there is an increase of impurities on MP-AC surface compared to the initial sample. This is because the adsorbate moves into the carbon pores during adsorption and results in the pore blockage (Basrur and Bhat, 2018). The surface elements of MP-AC determined using EDS is presented in Table 2.

Table 2. EDS analysis result of MP-AC before and after NH_3 adsorption

Sample	% mass			
	C	N	O	Other compounds
Before adsorption	71.84	16.07	8.77	3.32
After adsorption	70.62	16.94	9.43	3.01

Based on Table 2, the major compounds of MP-AC surface are carbon (71.84%), nitrogen (16.07%), and oxygen (8.77%). The N value of activated carbon

is higher than dried mangosteen peel (1-2.67%) (Devi et al., 2014; Giraldo and Moreno-Pirajan, 2018; Nasrullah et al., 2019), probably due to the use of N_2 as the inert atmosphere during the pyrolysis and cooling processes (Ahmad et al., 2013). Meanwhile, after the adsorption, there is no significant difference to these three major compounds.

3.4 Adsorption of NH_3

3.4.1 Effect of adsorbent mass and adsorbate concentration

The breakthrough curves of NH_3 adsorption at different adsorbent mass and adsorbate inlet concentration are presented in Figure 6.

Based on Figure 6, initially, NH_3 is fully adsorbed and adsorption process decreases with approaching equilibrium and gradually becomes constant. Figure 6(a) shows that for adsorbent mass of 1, 3, and 5 g, the equilibrium time was 16, 23, and 25 minutes respectively, indicating that saturation time becomes longer with the addition of adsorbent mass. This is due to the increasing surface area and available adsorption sites (Patel, 2019). Meanwhile, shown in Figure 6(b), smaller inlet concentrations produce the

longer breakthrough curves. According to [Ding and Liu \(2020\)](#) the decreasing inlet concentration

decreases the amount of gas molecule passing the adsorbent, so the active sites are exhausted slowly.

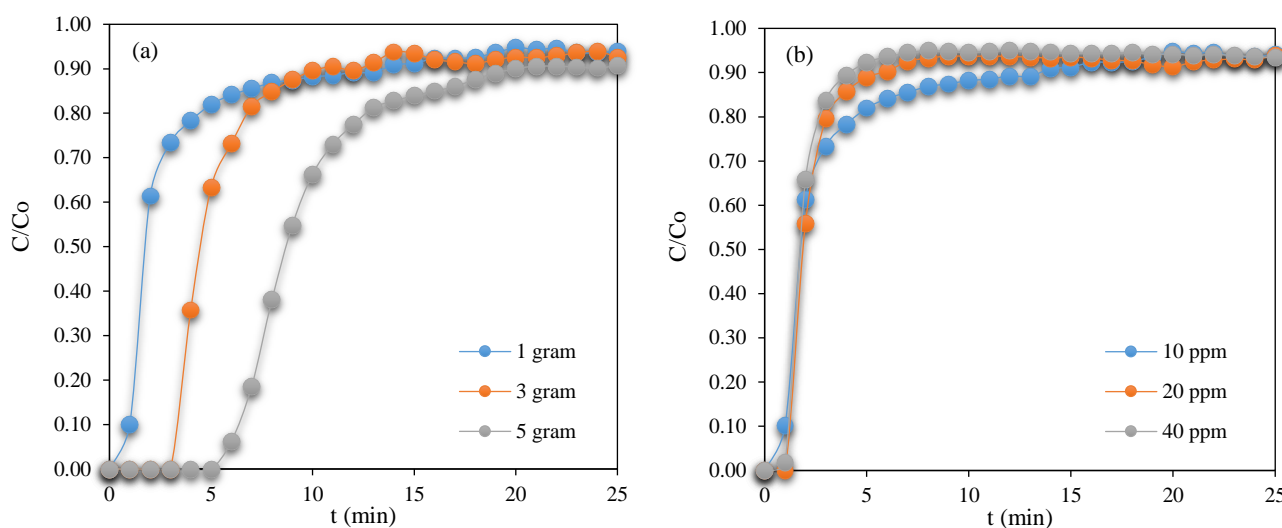


Figure 6. NH₃ breakthrough curve at different (a) adsorbent mass (10 ppm inlet concentration), and (b) different inlet concentration (adsorbent dosage 1 g/27.5 L)

3.4.2 Adsorption capacity

The adsorption capacity value is obtained from the breakthrough graph ([Figure 6](#)) which is calculated using Equation 4. The average NH₃ adsorption capacity on MP-AC is 0.41 mg/g. The value is lower compared to commercial activated carbon which ranges from 0.6 to 4.7 mg/g ([Ro et al., 2015](#)). This result correlates with the EDS result that the N compounds after and before adsorption do not show significant differences. The NH₃ adsorption may be affected by several factors such as surface functional group, pore size and structure, and surface area ([Kang et al., 2020](#); [Yeom and Kim, 2017](#)). Suspected in this study, acidic oxygen functional groups such as –OH, –NH, –C=O, –COOH, and metal ions is the main factor affecting adsorption capacity ([Ro et al., 2015](#); [Kang et al., 2020](#)). According to the FTIR result, some of acidic surface oxygen groups are present such as –OH and –C=O. However, the nitrile group is also found, thus increasing the basic nature of the activated carbon, as supported from the EDS result that the %mass of nitrogen can increase the basicity of the activated carbon ([Ahmad et al., 2013](#)). This finding might indicate that the surface of MP-AC is less acidic in nature due to the use of physical activation method ([Nowicki et al., 2015](#)) thus affecting the adsorption capacity. Additionally, further research is needed to enhance the NH₃ adsorption capacity and the use in numerous environmental applications.

3.4.3 Adsorption kinetics

Lagergren pseudo-first and pseudo-second order kinetic models are evaluated to describe the mechanism of NH₃ adsorption due to their good applicability in most cases ([Ghasemi et al., 2014](#)). The equations of pseudo-first order and pseudo-second order can be expressed as follows ([Lagergren, 1898](#); [Ho and McKay, 1999](#));

$$q_t = q_e[1 - e^{(-kt)}] \quad (6)$$

$$q_t = \frac{k_2 q_e^2 t}{1 + k_2 q_e^2 t} \quad (7)$$

Where; q_e and q_t (mg/g) are the adsorption capacity at equilibrium and time t , respectively; k and k_2 is the pseudo first and second order rate constant, respectively.

The results of kinetic parameters for each kinetic model are presented in [Table 3](#).

For determining the appropriate kinetic model, calculated q_e and R^2 values should be taken into account ([Unugul and Nigiz, 2020](#)). According to the results in [Table 3](#) and [Figure 7](#), both pseudo-first order and pseudo-second order kinetic models show high and good R^2 values. However, from the calculated q_e value, the pseudo-first order kinetic model is close to the experiment data. This indicates that the pseudo-first order kinetic model is more suitable to describe the adsorption mechanism where NH₃ adsorption is

physically controlled. The physisorption occurs due to the Van der Waals forces (Guo et al., 2005) and in the

pore surfaces which contain hydroxyl group as a preferred site to bind NH_3 (Yeom and Kim, 2017).

Table 3. Kinetics parameter of NH_3 adsorption on MP-AC

Mass (g)	Co (ppm)	qe exp (mg/g)	Pseudo-first order			Pseudo-second order		
			k_1 (min^{-1})	q_{e1} (mg/g)	R^2	k_2 ($\text{g}/\text{min} \cdot \text{mg}^{-1}$)	q_{e2} (mg/g)	R^2
1	10	0.413	0.205	0.404	0.971	0.394	0.516	0.986
	20	0.303	0.565	0.290	0.991	1.909	0.347	0.999
	40	0.316	0.793	0.309	0.996	2.507	0.370	1.000
3	10	0.363	0.231	0.345	0.988	0.619	0.417	0.992
	20	0.450	0.201	0.475	0.996	0.259	0.650	0.992
	40	0.448	0.306	0.474	0.993	0.415	0.637	0.987
5	10	0.427	0.134	0.441	0.994	0.204	0.586	0.986
	20	0.493	0.124	0.581	0.989	0.106	0.857	0.983
	40	0.515	0.169	0.612	0.989	0.135	0.908	0.984

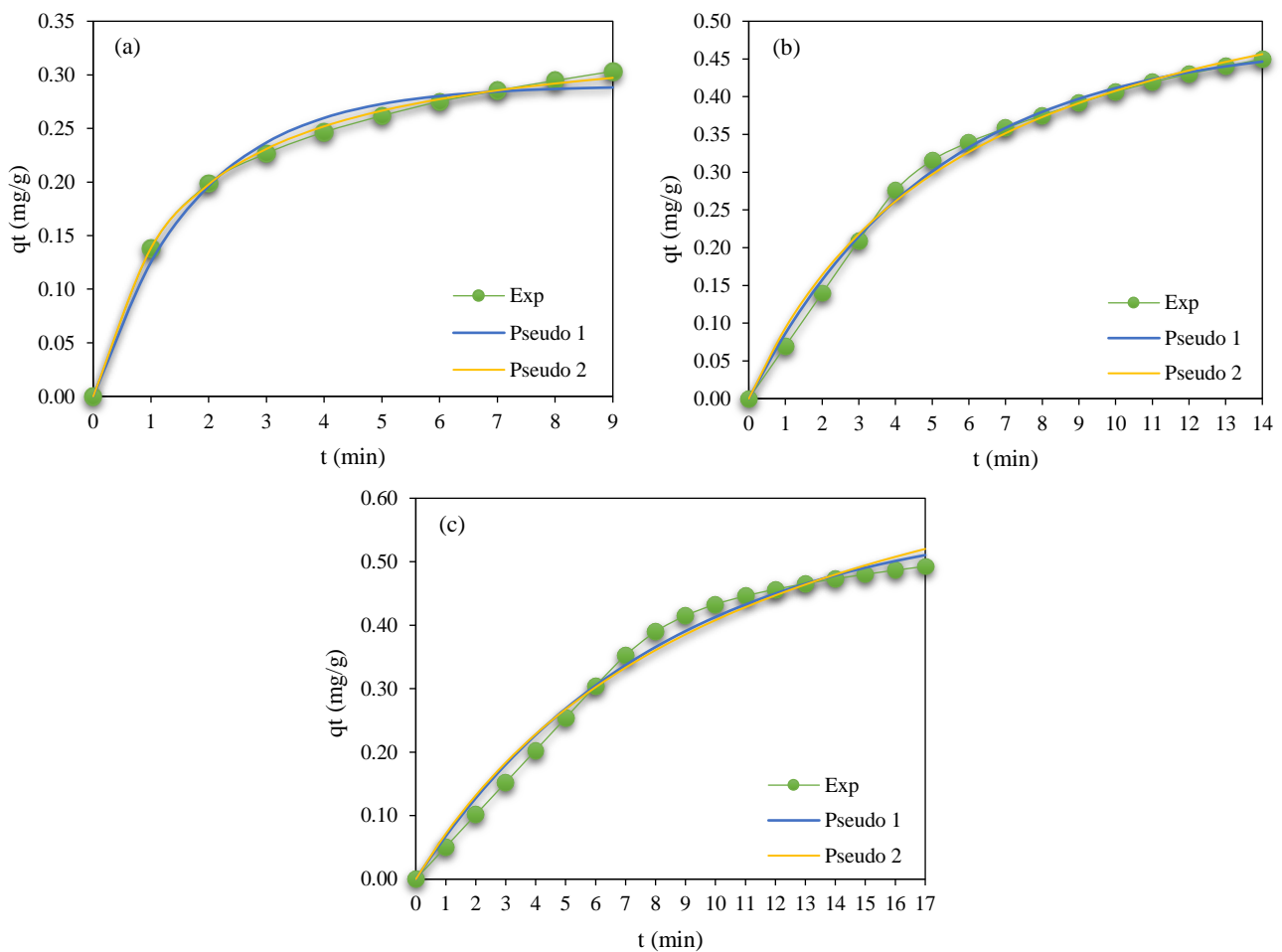


Figure 7. Adsorption kinetics of NH_3 on MP-AC at 20 ppm inlet concentration and adsorbent mass of (a) 1 g, (b) 3 g, and (c) 5 g

3.4.4 Adsorption isotherm

In this study, to describe the interaction between adsorbate and adsorbent at the equilibrium, the Freundlich and Langmuir isotherm were investigated. The linear equation of Freundlich and Langmuir isotherm model is shown in Equation 8 and 9

respectively as follows (Freundlich, 1906; Langmuir, 1917):

$$\log q_e = \log K_F + \frac{1}{n} \log C_e \quad (8)$$

$$\frac{C_e}{q_e} = \frac{C_e}{q} + \frac{1}{qK_L} \quad (9)$$

$$R_L = \frac{1}{1 + K_L \cdot C_e} \quad (10)$$

Where; q_e is the adsorption capacity at equilibrium (mg/g adsorbent), K_F is the Freundlich constant, K_L is the Langmuir constant (L/mg), n is the constant related to the adsorption energy of

heterogeneity adsorbent site, C_e is the concentration of contaminants in equilibrium (mg/L), and R_L is equilibrium parameter.

The values of isotherm parameters for both Freundlich and Langmuir isotherm models are presented in Table 4.

Table 4. Isotherm parameters of NH_3 adsorption on MP-AC

Mass	Freundlich				Langmuir			
	1/n	N	$K_f (\text{mg/g})(\text{L/mg})^{1/n}$	R^2	q (mg/g)	$K_L (\text{L/mg})$	R_L	R^2
1 g	0.195	5.1	0.15	0.615	0.297	820.63	0.09	0.992
3 g	0.153	6.5	1.22	0.644	0.481	611.00	0.12	0.994
5 g	0.146	6.8	1.10	0.877	0.557	544.21	0.13	0.999

Based on determination coefficient (R^2) from Table 4, the Langmuir isotherm is more suitable to describe the NH_3 adsorption process with the R^2 of 0.999. The similar result has also been reported in previous studies for Methylene Blue adsorption (Foo and Hameed, 2012; Nasrullah et al., 2019), and in the NH_3 adsorption on corncob activated carbon (Gebreegziabher et al., 2019). Langmuir isotherms indicates the monolayer adsorption where there is no interaction in adsorbate molecules (El maguana et al., 2020), and the carbon surfaces have homogeneous structures and identical active sites (Kutluay et al., 2019). Moreover, the equilibrium parameter (R_L) value is in the range of $0 < R_L < 1$, suggesting that the NH_3 adsorption using MP-AC is favorable (Hamzaoui et al., 2018).

4. CONCLUSION

MP-AC prepared from physical activation using CO_2 at 850°C for 120 min shows good porosity with surface area of $588.41 \text{ m}^2/\text{g}$, 6.07% moisture content, 9.8% ash content, and iodine number of 1153.69 mg/g . MP-AC can be used as an adsorbent material to remove NH_3 with adsorption capacity of 0.41 mg/g which is lower than commercial activated carbon ($0.6\text{--}4.7 \text{ mg/g}$). The pseudo-first order kinetic and the Langmuir isotherm are best fitted to the experimental data. Consequently, mangosteen peel may be potentially used as an activated carbon precursor with further modification for NH_3 adsorption and various environmental applications.

ACKNOWLEDGEMENTS

The authors would like to acknowledge Research Center for Nanoscience and Nano-

technology ITB for providing facilities in this research.

REFERENCES

- Ahmad F, Daud WMAW, Ahmad MA, Radzi R, Azmi AA. The effects of CO_2 activation, on porosity and surface functional group of cocoa (*Theobroma cacao*): Shell based activation carbon. Journal of Environmental Chemical Engineering 2013;1:378-88.
- Ahmad MA, Alrozi R. Optimization of preparation conditions for mangosteen peel-based activated carbons for the removal of Remazol Brilliant Blue R using response surface methodology. Chemical Engineering Journal 2010;165:883-90.
- Ahmad MA, Alrozi R. Removal of malachite green dye from aqueous solution using rambutan peel-based activated carbon: Equilibrium, kinetic, and thermodynamic studies. Chemical Engineering Journal 2011;171:510-6.
- Ambroz F, Macdonald TJ, Martis V, Parkin IP. Evaluation of the BET theory for the characterization of meso and microporous MOFs. Small Methods 2018;2:1800173.
- Basrur D, Bhat J. Preparation of activated carbon from mustard seed and its adsorption efficiency towards dye and acid. Journal of Urban and Environmental Engineering 2018; 12:266-76.
- Bernal V, Giraldo L, Moreno-Piraján J. Physicochemical properties of activated carbon: Their effect on the adsorption of pharmaceutical compounds and adsorbate-adsorbent interactions. Journal of Carbon Research 2018;4:62.
- Chandra TC, Mirna MM, Sunarso J, Sudaryanto Y, Ismadji S. Activated carbon from durian shell: Preparation and characterization. Journal of the Taiwan Institute of Chemical Engineering 2009;40:457-62.
- Chen Y, Huang B, Huang M, Cai B. On the preparation and characterization of activated carbon from mangosteen shell. Journal of the Taiwan Institute of Chemical Engineers 2011;42:837-42.
- Cheremisinoff PN, Ellerbusch F. Carbon Adsorption Handbook. Michigan, USA: Ann Arbor Science Publishers; 1978.
- Choo HS, Lau LC, Mohamed AR, Lee KT. Hydrogen sulfide adsorption by alkaline impregnated coconut shell activated carbon. Journal of Engineering Science and Technology 2013;8:741-53.

- Chung Y, Huang C, Liu CH, Bai H. Biotreatment of hydrogen sulfide- and ammonia-containing waste gases by fluidized bed bioreactor. *Journal of the Air and Waste Management Association* 2001;51:163-72.
- Crini G, Lichtfouse E. *Green adsorbents for Pollutant Removal: Innovative material*. Heidelberg, Germany: Springer; 2018.
- Devi AS, Latif PA, Tham YJ, Taufiq-Yap YH. Physical characterization of activated carbon derived from mangosteen peel. *Asian Journal of Chemistry* 2012;24:579-83.
- Ding S, Liu Y. Adsorption of CO₂ from flue gas by novel seaweed-based KOH-activated porous biochars. *Fuel* 2020;260:116382.
- Domingo-Garcia M, Groszek AJ, Lopez-Garzon FJ, Perez-Mendoza M. Dynamic adsorption of ammonia on activated carbons measured by flow microcalorimetry. *Applied Catalysis A: General* 2002;233:141-50.
- El maguana Y, Elhadiri N, Benchanaa M, Chikri R. Adsorption thermodynamic and kinetic studies of methyl orange onto sugar scum powder as a low-cost inorganic adsorbent. *Journal of Chemistry* 2020;2020:1-10.
- Foo KY, Hameed BH. Factors affecting the carbon yield and adsorption capability of the mangosteen peel activated carbon prepared by microwave assisted K₂CO₃ activation. *Chemical Engineering Journal* 2012;180:66-74.
- Fernandez ME, Nunell GV, Bonelli PR, Cukierman AL. Activated carbon developed from orange peels: Batch and dynamic competitive adsorption of basic dyes. *Industrial Crops and Products* 2014;62:437-45.
- Freundlich H. Over the adsorption in solution. *Journal of Physics Chemistry* 1906;57:385-470.
- Gebreegziabher TB, Wang S, Nam H. Adsorption of H₂S, NH₃, and TMA from indoor air using porous corn cob activated carbon: Isotherm and kinetic study. *Journal of Environmental Chemical Engineering* 2019;7:103234.
- Ghasemi M, Ghasemi N, Zahedi G, Alwi SRW, Goodarzi M, Javadian H. Kinetic and equilibrium study of Ni(II) sorption from aqueous solutions onto *Peganum harmala*-L. *International Journal of Environmental Science and Technology* 2014;11:1835-44.
- Giraldo L, Moreno-Piraján JC. CO₂ adsorption on activated carbon prepared from mangosteen peel. *Journal of Thermal Analysis and Calorimetry* 2017;133:337-54.
- Guo J, Xu WS, Chen YL, Lua AC. Adsorption of NH₃ onto activated carbon prepared from palm shells impregnated with H₂SO₄. *Journal of Colloid and Interface Science* 2005; 281:285-90.
- Hamzaoui M, Bestani B, Benderdouche N. The use of linear and nonlinear methods for adsorption isotherm optimization of basic green 4-dye onto sawdust-based activated carbon. *Journal of Materials and Environmental Sciences* 2018; 9:1110-8.
- Hastuti N, Pari G, Setiawan D, Mahpudin M, Godang DM. Acidity and alkalinity level of Mayan bamboo activated charcoal (MBAC) on saturated vapor of acid chloride and sodium hydroxide. *Widyariset* 2015;1:41-50.
- Ho YS, McKay G. Pseudo-second order model for sorption processes. *Process Biochemistry* 1999;34:451-65.
- Kang DW, Ju SE, Kim DW, Kang M, Kim H, Hong CS. Emerging porous materials and their composites for NH₃ gas removal. *Advanced Science* 2020;7:2002142.
- Kutluay S, Baytar O, Şahin Ö. Equilibrium, kinetic and thermodynamic studies for dynamic adsorption of benzene in gas phase onto activated carbon produced from *Elaeagnus angustifolia* seeds. *Journal of Environmental Chemical Engineering* 2019;7:102947.
- Lagergren S. About the theory of so-called adsorption of soluble substances. *Kungliga Svenska Vetenskapsakademiens Handlingar* 1898;24:1-39.
- Lan X, Jiang X, Song Y, Jing X, Xing X. The effect of activation temperature on structure and properties of blue coke-based activated carbon by CO₂ activation. *Green Processing and Synthesis* 2019;8:837-45.
- Langmuir I. The constitution and fundamental properties of solids and liquids. II. Liquids. *Journal of the American Chemical Society* 1917;3:1848-906.
- Li Y, Wang X, Cao M. Three-dimensional porous carbon frameworks derived from mangosteen peel waste as promising materials for CO₂ capture and supercapacitors. *Journal of CO₂ Utilization* 2018;27:204-16.
- Meneghetti E, Baroni P, Vieira RS, Da Silva MGC, Beppu MM. Dynamic adsorption of chromium ions onto natural and crosslinked chitosan membranes for wastewater treatment. *Material Research* 2010;13:89-94.
- Mukti NIF, Prasetyo I, Mindaryani A. Preparation of ethylene adsorbent by pyrolysis of mangosteen peels. *Proceeding of Indonesian National Seminar on Chemical Engineering 2015 Sustainable Energy and Mineral Processing for National Competitiveness*; 2015 Oct 12-13; Gadjah Mada University Club Hotel, Yogyakarta: Indonesia; 2015.
- Nasrullah A, Saad B, Bhat AH, Khan AS, Danish M, Isa MH, et al. Mangosteen peel waste as a sustainable precursor for high surface area mesoporous activated carbon: Characterization and application for methylene blue removal. *Journal of Cleaner Production* 2019;211:1190-200.
- Nor NM, Lau LC, Lee KT, Mohamed AR. Synthesis of activated carbon from lignocellulosic biomass and its applications in air pollution control: A review. *Journal of Environmental Chemical Engineering* 2013;1:658-66.
- Nowicki P, Kazmierczak J, Pietrzak R. Comparison of physicochemical and sorption properties of activated carbons prepared by physical and chemical activation of cherry stones. *Powder Technology* 2015;269:312-9.
- Patel H. Fixed bed column adsorption study: A comprehensive review. *Applied Water Science* 2019;9:1-17.
- Rangabhashiyam S, Balasubramanian P. The potential of lignocellulosic biomass precursors for biochar production: Performance, mechanism, and wastewater application. *Industrial Crops and Products* 2019;128:405-23.
- Rattanapan S, Pengjam P, Kongsune P. Preparation and characterization of mangosteen peel activated carbon. *Thaksin University Journal* 2014;17:13-21.
- Reza MS, Yun CS, Afroze S, Radenahmad N, Bakar MSA, Saidur R, et al. Preparation of activated carbon from biomass and its' applications in water and gas purification: A review. *Arab Journal of Basic and Applied Sciences* 2020;27:208-38.
- Ro KS, Lima IM, Reddy GB, Jackson MA, Gao B. Removing gaseous NH₃ using biochar as an adsorbent. *Agriculture* 2015;5:991-1002.
- Saka C. BET, TG-DTG, FT-IR, SEM, iodine number analysis and preparation of activated carbon from acorn shell by chemical activation with ZnCl₂. *Journal of Analytical and Applied Pyrolysis* 2012;95:21-4.
- Saputro EA, Wulan VDR, Winata BY, Yogaswara RR, Erliyanti NK. The process of activated carbon from coconut shells

- through chemical activation. *Journal of Science and Technology* 2020;9:23-9.
- Statistics Indonesia (BPS). *Statistics of Annual Fruit and Vegetable Plants Indonesia 2018*. Jakarta, Indonesia: BPS-Statistics Indonesia; 2019.
- Unugul T, Nigiz FU. Preparation and characterization an active carbon adsorbent from waste mandarin peel and determination of adsorption behavior on removal of synthetic dye solutions. *Water, Air and Soil Pollution* 2020;231:538.
- Xu R, Tian H, Pan S, Prior SA, Feng Y, Batchelor WD, et al. Global ammonia emissions from synthetic nitrogen fertilizer applications in agricultural systems: Empirical and process-based estimates and uncertainty. *Global Change Biology* 2019;25:314-26.
- Vohra M. Treatment of gaseous ammonia emissions using date palm pits based granular activated carbon. *International Journal of Environmental Research and Public Health* 2020;17:1519.
- Yang T, Lua AC. Characteristics of activated carbons prepared from pistachio-nut shells by physical activation. *Journal of Colloid and Interface Science* 2003;267:408-17.
- Yani M, Nurcahyani PR, Rahayuningsih M. Ammonia removal by biofilter technique packed with coral and granulated activated carbon (GAC) inoculated with enriched nitrifying bacteria. *Journal of Agroindustrial Technology* 2013;23:22-9.
- Yeom C, Kim Y. Adsorption of ammonia using mesoporous alumina prepared by a templating method. *Environmental Engineering Research* 2017;22:401-6.
- Yuliusman, Nasruddin, Afdhol MK, Haris F, Amiliana RA, Hanafi A, et al. Production of activated carbon from coffee grounds using chemical and physical activation method. *Advanced Science Letters* 2017;23:5751-5.